

## Preparation of double-raschel knitted silk vascular grafts and evaluation of short-term function in a rat abdominal aorta

Takahito Yagi · Michiko Sato · Yasumoto Nakazawa ·  
Kimie Tanaka · Masataka Sata · Kenji Itoh ·  
Yoshihide Takagi · Tetsuo Asakura

Received: 18 October 2010 / Accepted: 19 January 2011 / Published online: 23 February 2011  
© The Japanese Society for Artificial Organs 2011

**Abstract** Silk fibroin fiber has a long history of use in sutures because of its high strength and toughness. In the work reported in this paper, small-diameter vascular grafts 1.5 mm in diameter and 10 mm in length were prepared by coating a double-raschel knitted silk fiber graft with silk fibroin aqueous solution containing poly(ethylene glycol diglycidyl ether) as a cross-linking agent. The most important character of silk fibroin graft is remodeling, which is never observed for polyester fiber or expanded polytetrafluoroethylene grafts. The double-raschel knitted silk fiber graft with coating has sufficient physical strength and protects the ladder from the end in the implantation process. The coating also gives protection against leakage

of blood from the graft, and elasticity to the graft. Eight weeks after implantation of the grafts in rat abdominal aorta, early formation of thrombosis was avoided.

**Keywords** Silk fibroin fiber · Small-diameter vascular graft · Double-raschel knitting

### Introduction

Vascular grafts prepared from expanded polytetrafluoroethylene (ePTFE) or poly(ethylene terephthalate) (Dacron) have been used clinically for many years for the revascularization of blood vessels with inner diameters  $\geq 6$  mm. However, replacement of vessels with these synthetic materials for smaller vessels  $< 5$  mm, leads to the failure of such grafts, mainly because of early thrombosis formation [1, 2]. In addition, such synthetic materials that are commonly used lack growth potential, and long-term results have revealed several material related failures, for example stenosis, thromboembolization, calcium deposition, and infection [2]. To overcome these limitations, various tissue-engineered vascular grafts have been developed, for example poly-L-lactic acid, polyglycolic acid, polyurethane, poly- $\epsilon$ -caprolactone, cellulose, chitosan, poly(vinyl alcohol) together and their composites [1, 3–8]. However, at present, no materials satisfy the severe requirements of small-diameter grafts.

As a natural fiber, silk fibroin from *Bombyx mori* is one biomaterial candidate for small-diameter artificial grafts, because silk fibroin fiber has a long history of use in sutures because of its high strength and toughness [9]. In our previous studies, silk fibroin grafts proved to be efficient as vascular grafts implanted in rat models [10]. A small vessel (1.5 mm in diameter, 10 mm in length) was prepared by

---

T. Yagi · M. Sato · Y. Nakazawa · T. Asakura (✉)  
Department of Biotechnology, Tokyo University of Agriculture  
and Technology, 2-24-16 Nakacho, Koganei,  
Tokyo 184-8588, Japan  
e-mail: asakura@cc.tuat.ac.jp

Y. Nakazawa  
Nature and Science Museum,  
Tokyo University of Agriculture and Technology,  
2-24-16 Nakacho, Koganei, Tokyo 184-8588, Japan

K. Tanaka  
Department of Cardiovascular Medicine,  
The University of Tokyo, 7-3-1 Hongo, Bunkyo-ku,  
Tokyo 113-8655, Japan

M. Sata  
Department of Cardiovascular Medicine, Institute of Health  
Biosciences, The University of Tokushima Graduate School,  
3-18-15, Kuramotocho, Tokushima, Tokushima 770-8503, Japan

K. Itoh · Y. Takagi  
Fukui Warp Knitting Co., Ltd, 3-519-3 Nishikaihatsu,  
Fukui, Fukui 910-8512, Japan

repeated braiding and winding of the fibers. Tubes were then coated with silk fibroin gel and implanted into the rat abdominal aorta. Patency of fibroin grafts 1 year after implantation was significantly higher than that of PTFE grafts used as control (85.1 vs. 30%,  $P < 0.01$ ). Endothelial cells and smooth muscle cells migrated into the fibroin graft early after implantation and organized endothelial and medial layers, as determined by anti-CD31 or anti- $\alpha$ -smooth muscle actin immunostaining. Total number of SMCs increased 1.6-fold from 1 to 3 months. Vasa vasorum was also formed in adventitia. Sirius-red staining revealed that the collagen content of fibroin grafts significantly increased 1 year after implantation, with a decrease in fibroin content. Thus, silk fibroin might be a promising material to engineer vascular prostheses for small arteries. Silk fibroin grafts, especially, can be used as a remodeling graft, which is never observed for polyester or PTFE grafts. However, there are some problems. The most serious problem is that silk fibroin grafts tend to fray from the end as a result of oblique or longitudinal cutting of the grafts. In addition, the strength of the graft is much weaker than PTFE or polyester fiber grafts. These problems are expected to be overcome by improvement of the process of preparation of silk fibroin fiber grafts. This is especially important when we use the silk fibroin graft for large animals, for example dogs or pigs. To develop small-diameter silk fibroin vascular grafts, several improvements of these problems from the previous silk graft is required. Thus, the strength should be stronger, while maintaining elasticity, and leakage of blood from the graft tube should be prevented, as also should fraying from the end of the graft.

In the work reported in this paper, silk fibroin grafts 1.5 mm in diameter and 10 mm in length were prepared by combination of the double-raschel knitted silk fiber graft and coating with silk fibroin aqueous solution containing poly(ethylene glycol diglycidyl ether) (PGDE) as cross-linking agent. Double-raschel knitting has been usually used for preparation of vascular grafts of polyester fiber; preparation of grafts with silk fibroin fiber was performed for the first time in this work. In double-raschel knitting, and the thickness or elasticity can be changed by changing the knitting. It was considered that we can control the physical or mechanical characteristics of the vascular graft by using different types of double-raschel knitting. In the work reported in this paper, three kinds of double-raschel knitted bases were used. We compared small-diameter vascular grafts based these types of double raschel knitting and estimated which type was suitable for small-diameter vascular grafts. The double-raschel knitted silk fiber graft was shown to have sufficient strength, to prevent fraying from the end in the implantation process, and to prevent slight leakage of blood from the graft. By implantation of

the graft in the rat abdominal aorta, it was shown that early formation of thrombosis could be avoided.

## Materials and methods

### Materials

Raw silk fibers with silk sericin were used as the starting materials. The tube of the silk vascular graft of 1.5 mm diameter was prepared by use of a computer-controlled double-raschel knitting machine. Three kinds of tubes, ①–③ were prepared by changing the double-raschel knitted procedures. Scanning electron microscope (SEM; VE-7800; Keyence, Tokyo, Japan) images of the surfaces of these silk tubes are shown in Fig. 1, together with the knitting procedure shown as two lines colored by red and black. In our experiments, these three kinds of the silk graft tubes of 1.5 mm diameter were used and compared with each other. These double-raschel knitted silk tubes were then degummed in a mixture of sodium carbonate (0.1% w/v) and Marseille soap (0.2% w/v) solution at 95°C for 120 min to remove silk sericin from the surface of the silk fibroin fiber. This degumming process was repeated three times. Removal of silk sericin was confirmed by SEM. A poly(vinyl chloride) rod was inserted into the silk fibroin graft tube so the surface of the rod was covered with the silk fibroin fiber. The tubes were then coated with silk fibroin aqueous solution containing PGDE as cross-linking agent. The coated tubes were frozen at  $-80^{\circ}\text{C}$  overnight. To remove unreacted PGDE, the tubes were immersed in distilled water for 4 days and dried. After these treatments, the coating layer on the silk fibroin vascular graft was spongy in nature. The silk fibroin grafts were sterilized in an autoclave at  $120^{\circ}\text{C}$  for 20 min. The grafts were hydrated in 0.9% saline solution for 60 min before in-vivo and in-vitro experiments.

### Measurement of physical properties

The permeability of the graft tube was determined in accordance with ISO7198. A water reservoir was connected to a polyethylene tube followed by the silk fibroin graft. The water reservoir was set so the hydrostatic pressure applied to the graft was approximately 120 mmHg. The water permeating through the graft wall was collected and calculated in  $\text{ml}/\text{min}/\text{cm}^2$ . Ten specimens were tested for each double-raschel tube.

Circumferential tensile strengths of the silk fibroin grafts were measured by use of a test machine (EZ graph; Shimadzu, Kyoto, Japan). Ten dry, short, ring-shaped specimens with an axial length of 10 mm were prepared for each double-raschel tube and the outer diameters were measured. The load cell was 5 N and rate of stretching was

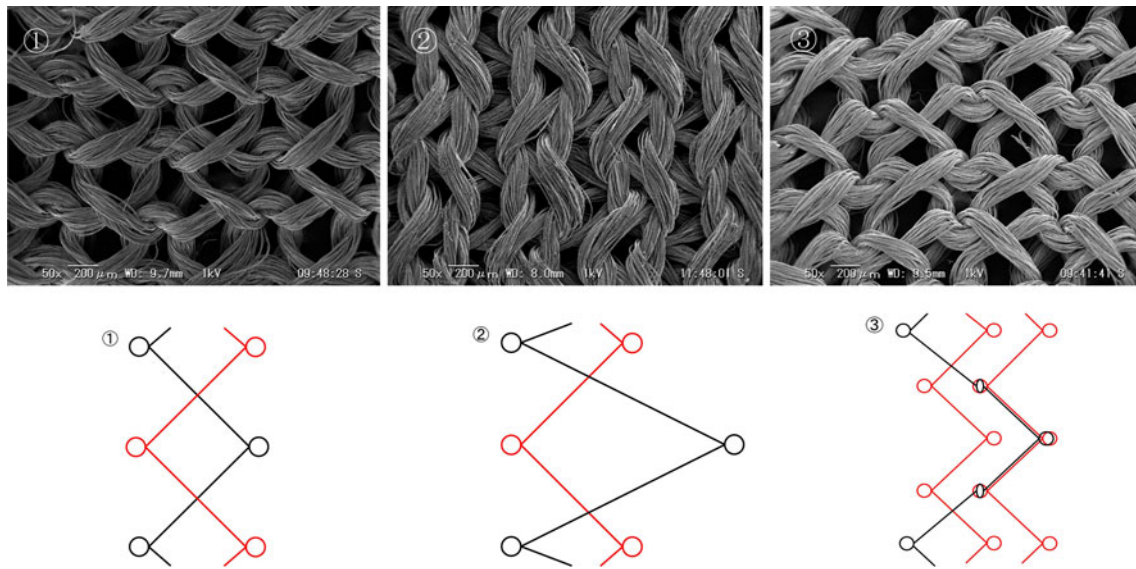


**Fig. 1** SEM images and schemes of three kinds of double-raschel knitting. Graft ① is the basic knitting, and the thinnest type of knitting. Grafts ② and ③ were more complex types of knitting than

graft ①. Graft ② has closer mesh and the graft ③ is thicker than the graft ①. The knitting procedures are shown with two lines colored *red* and *black*



**Fig. 2** SEM image of coated fabricated silk fibroin graft

2 mm/min. The load applied to the specimen before failure was divided by the effective cross-sectional area (which was defined by  $2 \times \text{wall thickness} \times \text{length of the ring-shaped specimen}$ ). The tensile strength was measured as a function of stroke distance.

The circumferential compressive elastic modulus of the silk fibroin graft tube was also tested. The test machine is the same as that used for tensile strength. Ten short, ring-shaped specimens with an axial length of 10 mm were also prepared for each tube and the outer diameters were measured. Specimens were also hydrated in a saline solution for 1 h before testing. The road cell was 5 N and rate of compression was 2 mm/min. The compressive strength

when the specimen was compressed by 10% of the value of the inner diameter was measured.

Ten specimens for each double-raschel tube were also used for anti-kinking experiments. The specimens were hydrated in a saline solution for 1 h before testing. The silk fibroin graft tube was formed into a loop and both ends of the graft were pulled in order to reduce the size of loop until the kink radius was measured. The minimum radius of the loop at which the graft was not kinked was measured by use of cylindrical mandrels of known diameter ranging from 5 mm to 40 mm.

#### In-vivo experiments with rats

##### *Surgical procedure*

Male Sprague–Dawley (SD) rats weighing 400–500 g were purchased from SLC (Shizuoka, Japan). All rats were kept in microisolator cages with a 12-h light/dark cycle. All experimental procedures and protocols were approved by the Animal Care and Use Committee of the University of Tokyo and complied with the *Guide for the care and use of laboratory animals* (National Institutes of Health publication No. 86-23, revised 1985).

A silk fibroin graft (7 mm long, 1.5 mm inner diameter) was implanted into the rat abdominal aorta, which had a diameter of approximately 1.5 mm. Rats were anesthetized by intraperitoneal injection of pentobarbital (50 mg/kg body weight). The abdominal aorta was exposed and the aortic branches in this segment were ligated. After an intravenous injection of heparin (100 IU/kg), the proximal

**Fig. 3** Permeabilities of several silk fibroin vascular grafts. The values reported for the sealed polyester prostheses, polyesters A and B, are also shown for comparison

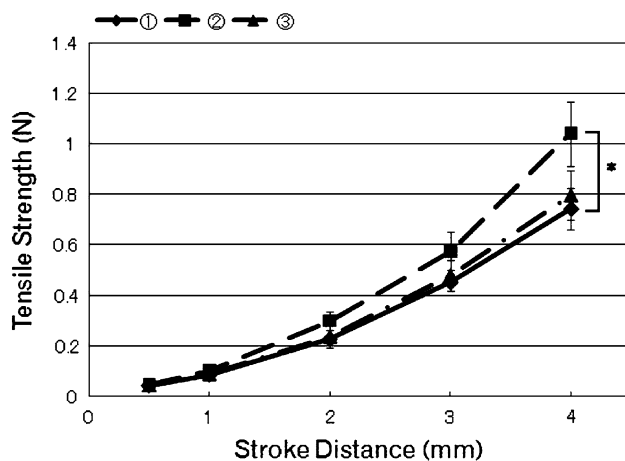
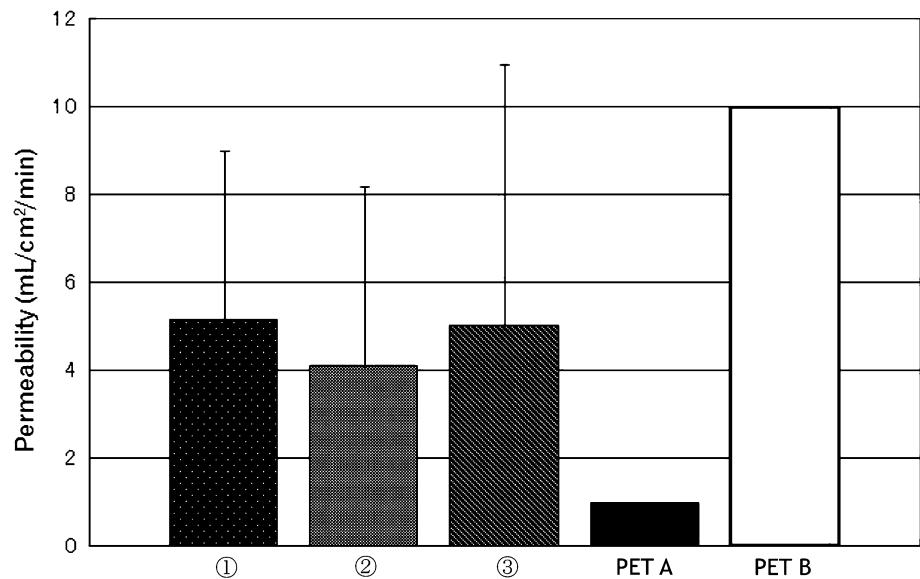


**Fig. 4** Changes of circumferential tensile strength of three kinds of double-raschel bases ①–③ before coating. The lower value was interpreted as higher elasticity. (\* $P < 0.05$ )

and distal portions of the infrarenal aorta were clamped. A 7-mm segment of aorta was removed and replaced by a fibroin graft by end-to-end anastomosis using interrupted 9-0 monofilament nylon sutures (BEAR, Ibaraki, Japan), starting with two stay sutures at 180° to each other, then suturing the front wall, followed by the back wall. Each anastomosis required 8–10 stitches. The distal, then the proximal vascular clamps were slowly removed, and flow was restored through the fibroin graft.

Graft patency was monitored by color Doppler imaging and pulse waves recorded with a 12-MHz sector probe and an echo-imaging apparatus (EnVisor M25040A; Phillips, Tokyo, Japan) at 2 and 8 weeks before sacrifice, under anesthesia with pentobarbital. Blood flow velocity was

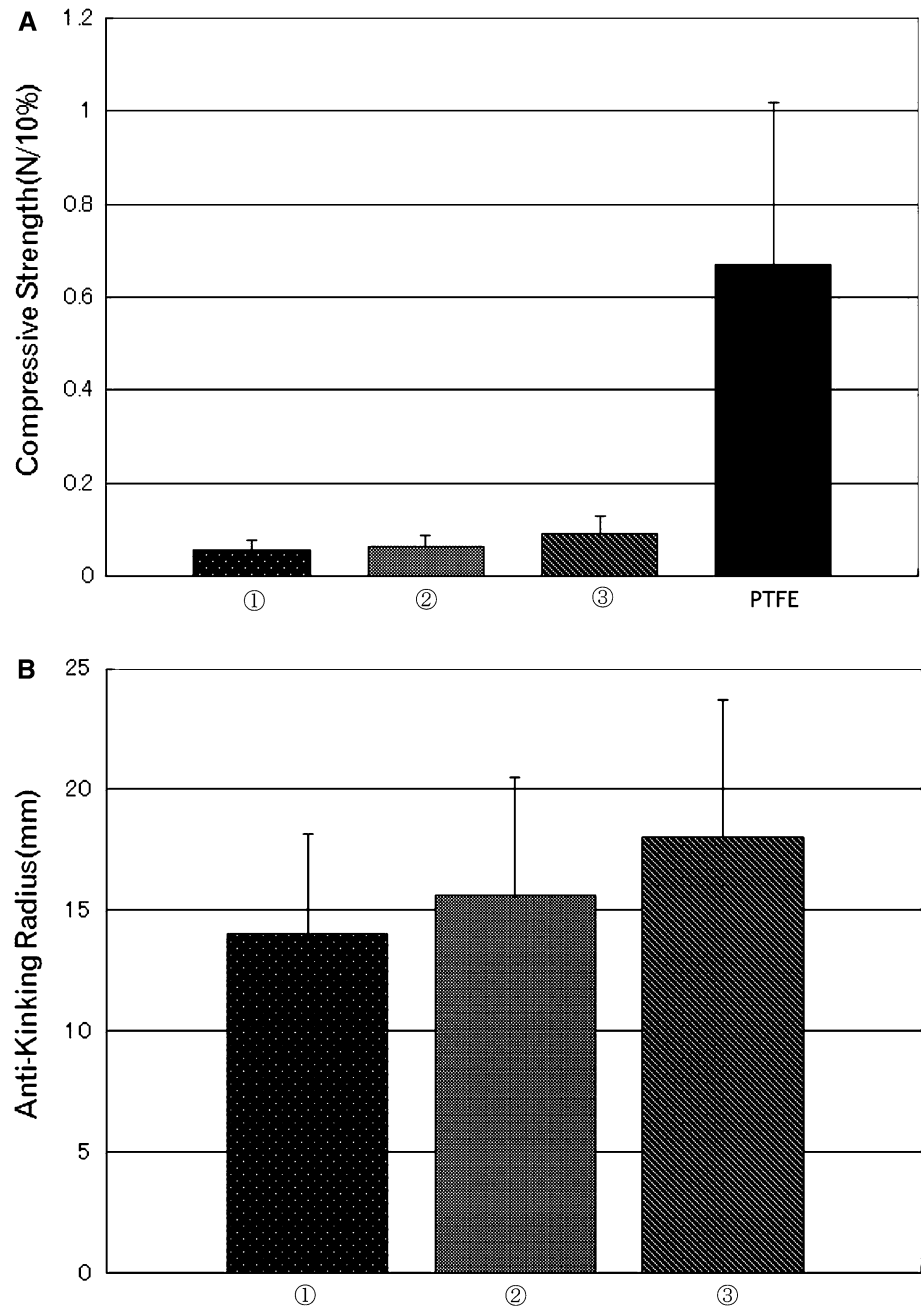
measured. Signs of thrombosis and aneurysm formation were carefully checked ( $N = 4-5$ ).

#### *Histologic and immunohistologic examination*

Before euthanasia, rats underwent a general physical examination to evaluate their condition. At death, the rats were perfused with 0.9% saline solution through the left ventricle. The grafts were carefully removed with surrounding tissue, cut transversely in the midline into two pieces, and fixed in methanol for histologic analyses. Methanol-fixed samples were embedded in paraffin. Paraffin-embedded sections (4  $\mu$ m thick) were processed for hematoxylin and eosin staining. The sections were incubated with primary antibodies, including alkaline phosphatase conjugated anti- $\alpha$ -smooth muscle actin (SMA; clone 1A4; Sigma-Aldrich, St Louis, MO, USA), anti-rat CD31 (clone TLD-3A12; BD Biosciences, San Jose, CA, USA), followed by incubation with biotinylated anti-mouse immunoglobulin (Ig) G secondary antibody (Dako, Glostrup, Denmark) and subsequent use of the avidin-biotin complex technique and Vector Red substrate (Vector Laboratories, Burlingame, CA, USA). Nuclei were counterstained with hematoxylin. All in-vivo tests were performed as previously reported [10].

All of the graft, and the anti-CD31-stained luminal surface perimeter of the cross-section of the silk fibroin vascular graft at anastomosis, near to the anastomosis (approx. 1 mm from the end of the graft) and the mid-portion of graft (approx. 3 mm from the end of the graft) were measured. The length of the stained graft wall was calculated for all the grafts and the value was regarded as endothelial cells coverage. The endothelial cells coverage was compared among the three kinds of

**Fig. 5** Compressive strength (a) and anti-kinking radius (b). No significant differences among three kinds of silk fibroin grafts were observed for compressive strength. The reported compressive strength of PTFE was also shown [12]. The anti-kinking radius tends to small in the order ①, ②, ③



the double-raschel silk fibroin vascular grafts 2 and 8 weeks after implantation.

The thickness of the intimal smooth muscle layer which was stained with anti- $\alpha$ -smooth muscle actin was measured at three different points of the cross-section of the double-raschel silk fibroin vascular graft at random and averaged over these three points. This value was regarded as intimal hyperplasia marker. Intimal thickening on anastomosis, near to the anastomosis and at midportion sites of the three kinds of the double-raschel silk fibroin vascular grafts were compared.

Cellular in-growth tissue infiltration was defined as the percentage of the graft wall area which was densely penetrated by host cells, mostly from the outside toward the inside [11]. In the hematoxylin and eosin (H&E) stained cross-sections, silk fibroin was stained more deeply than tissue derived from host cells. A part of the graft wall was extracted from the overall picture of the H&E-stained cross-section and the area was measured. The silk fibroin area was eliminated and just the tissue area was measured. The extent of the tissue area for silk fibroin + tissue area was calculated. All histological and immunohistological

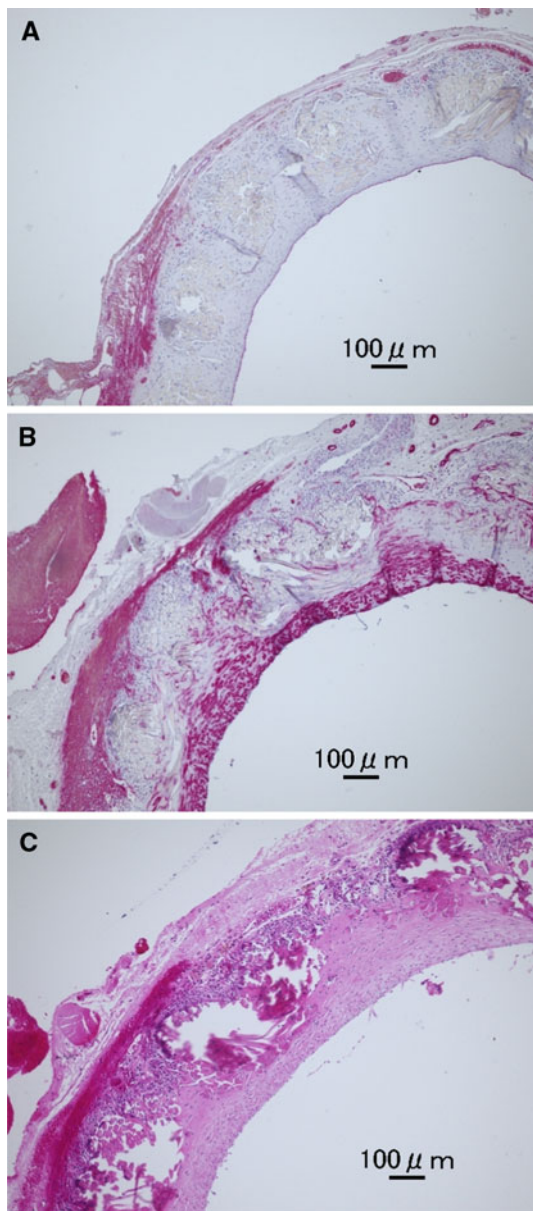


**Fig. 6** Histological and Immunohistological staining images of the midportion of the cross-sections of graft ① as an example. The cross-sections of the silk fibroin graft 8 weeks after implantation stained with anti-CD31 (a), anti- $\alpha$ -SMA (b) antibody and H&E stained (c)

stained images were analyzed by use of a Keyence BZ-9000 microscope and analytical software supplied with the product.

#### Statistical analysis

Results obtained from physical property tests and tissue growth by immunohistological or histological staining were evaluated statistically by analysis of variance. Results

are given as mean  $\pm$  SD. Values of  $P < 0.05$  were considered significant.

## Results

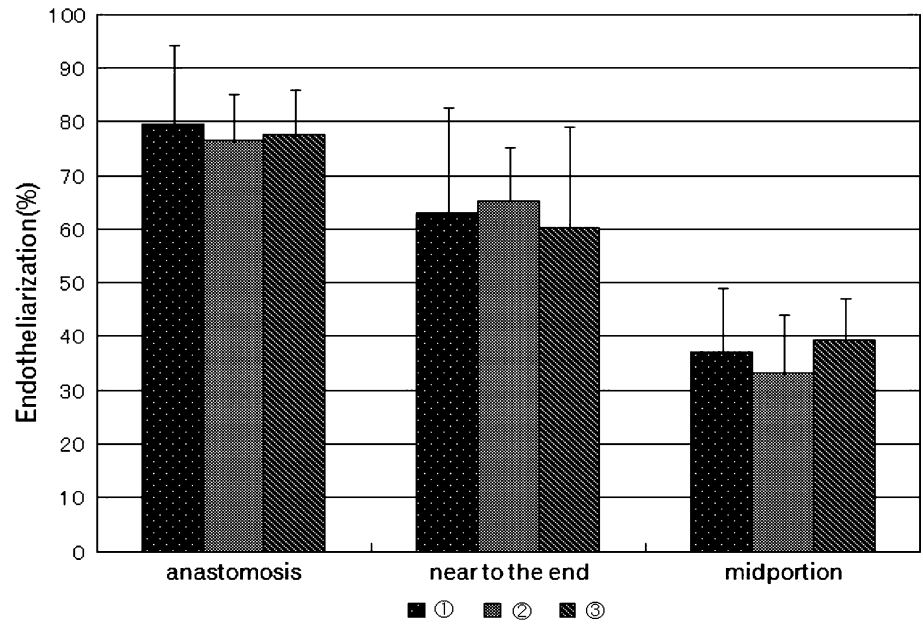
### Characterization of the fabricated double-raschel silk fibroin vascular grafts after coating

Figure 2 shows the typical SEM image of the inner part of the fabricated double-raschel silk fibroin vascular grafts after coating. The silk fibroin fibers are still observed because of the thin coating. However, large open spaces among the bunches of fibers observed in Fig. 1 for uncoated tubes were buried. This character of the surface was essentially the same among all three kinds of double-raschel silk graft after coating. The graft wall thickness was approximately 300  $\mu$ m in the wet state and approximately 250  $\mu$ m in the dry state.

The water permeabilities of the three kinds of coated double-raschel silk fibroin grafts ①–③ are summarized in Fig. 3 together with two corresponding values reported in the specification of two commercial sealed polyester vascular prostheses, PET A (Triprex; Terumo, Tokyo) and PET B (J Graft sealed; Junken Medical, Tokyo) [12]. The permeabilities of grafts ①–③ were  $5.2 \pm 3.9$ ,  $4.1 \pm 4.1$ , and  $5.0 \pm 6.0$  mL/cm<sup>2</sup>/min, respectively. Although the experimental error is relatively large, we believe the seal of these silk fibroin grafts is sufficiently good as a result of comparison with values for commercial sealed polyester vascular prostheses. There are no significant differences among the three kinds of silk fibroin grafts.

Plots of the tensile strength of the three kinds of silk fibroin double-raschel bases before coating, as a function of stroke distance, are shown in Fig. 4. In these experiments, a slower increase of tensile strength with increasing stroke distance means more elasticity. There is no significant difference between bases ① and ③, but the graft base ② is clearly stiffer than other two. The compressive strength when the samples were compressed to 10% of the inner diameter is summarized in Fig. 5a. A value reported [13] for a PTFE prosthesis is also shown (the trade name was not given in the paper). Thus the compressive strengths of the silk fibroin grafts are much lower than that for the PTFE prosthesis. The minimum radius of the loop for which the graft was not kinked is shown in Fig. 5b. The values for ①, ②, and ③ were  $14.0 \pm 4.2$ ,  $15.6 \pm 4.9$ , and  $18.0 \pm 5.7$  mm, respectively. The same tendencies were observed between the kink radius and the compressive strength values among three silk fibroin grafts, i.e. graft ① had the highest elasticity and flexibility although the difference is small among the three grafts.

**Fig. 7** Endothelial cell coverage at anastomosis (*anastomosis*), approximately 1 mm from the end (*near to the end*), and approximately 3 mm from the end (*midportion*) for the three kinds of double-raschel bases 2 weeks after implantation



**Fig. 8** At 8 weeks after implantation, luminal surfaces were covered with endothelial cells completely for almost all the silk fibroin grafts

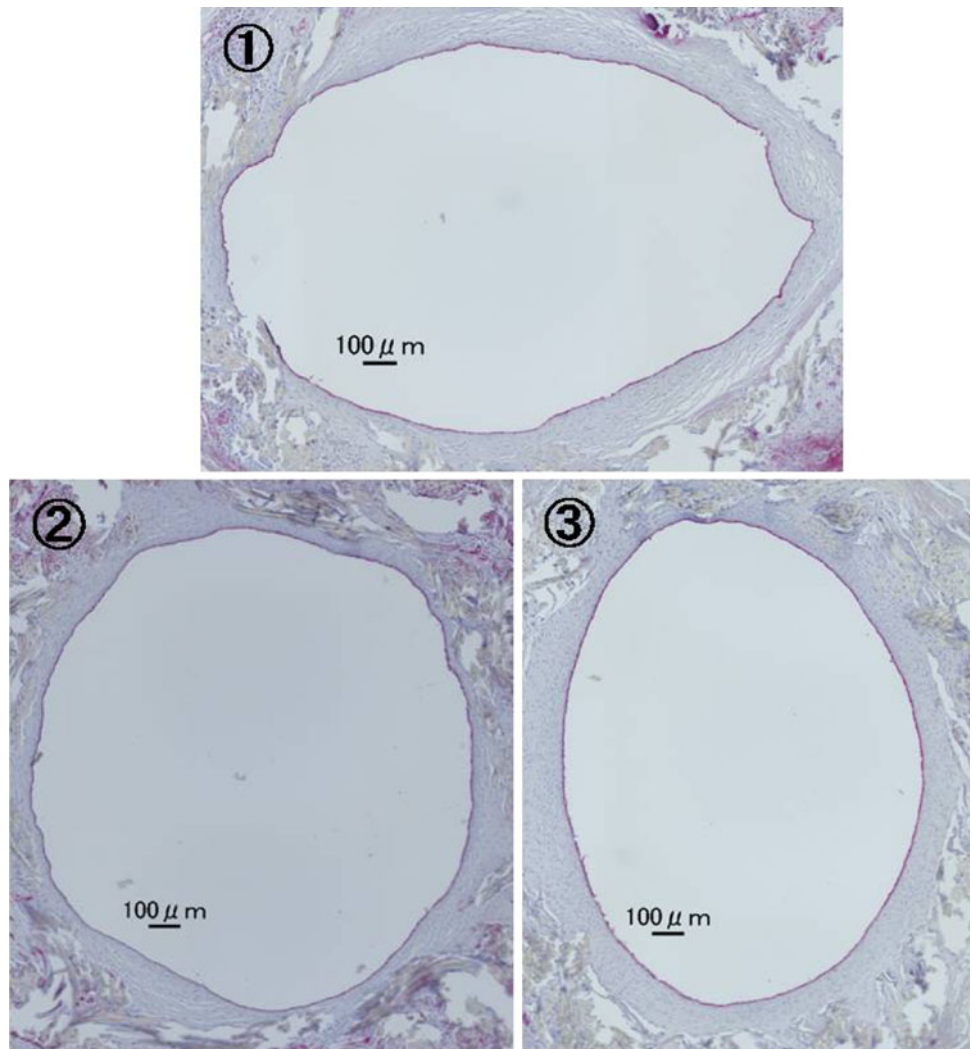
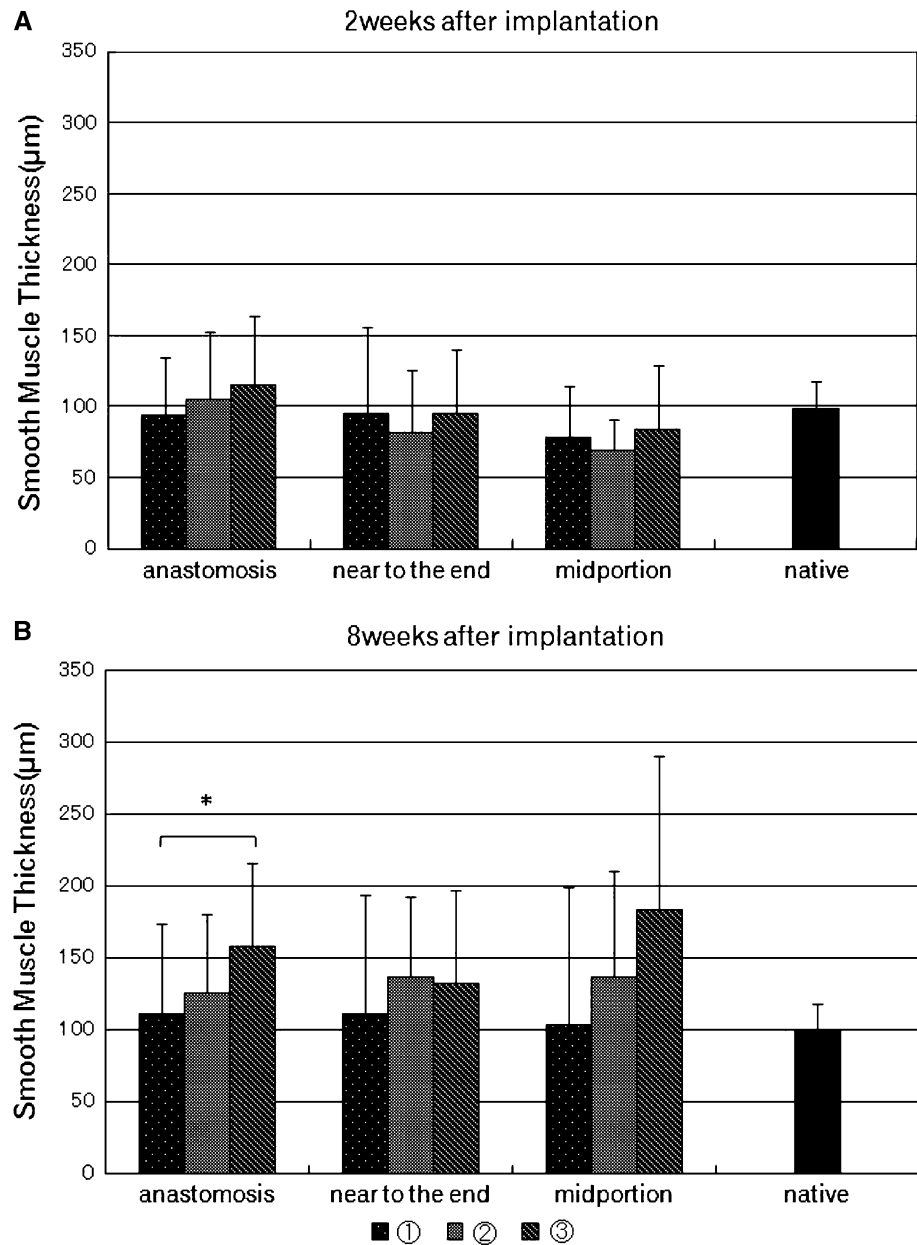


**Fig. 9** Thickness of smooth muscle layers at the anastomosis (*anastomosis*), approximately 1 mm from the end of the anastomosis (*near to the end*), and approximately 3 mm from the end of the anastomosis (*midportion*) for the three kinds of double-raschel bases 2 and 8 weeks after implantation. The thickness of the smooth muscle layer of the native aorta is also shown



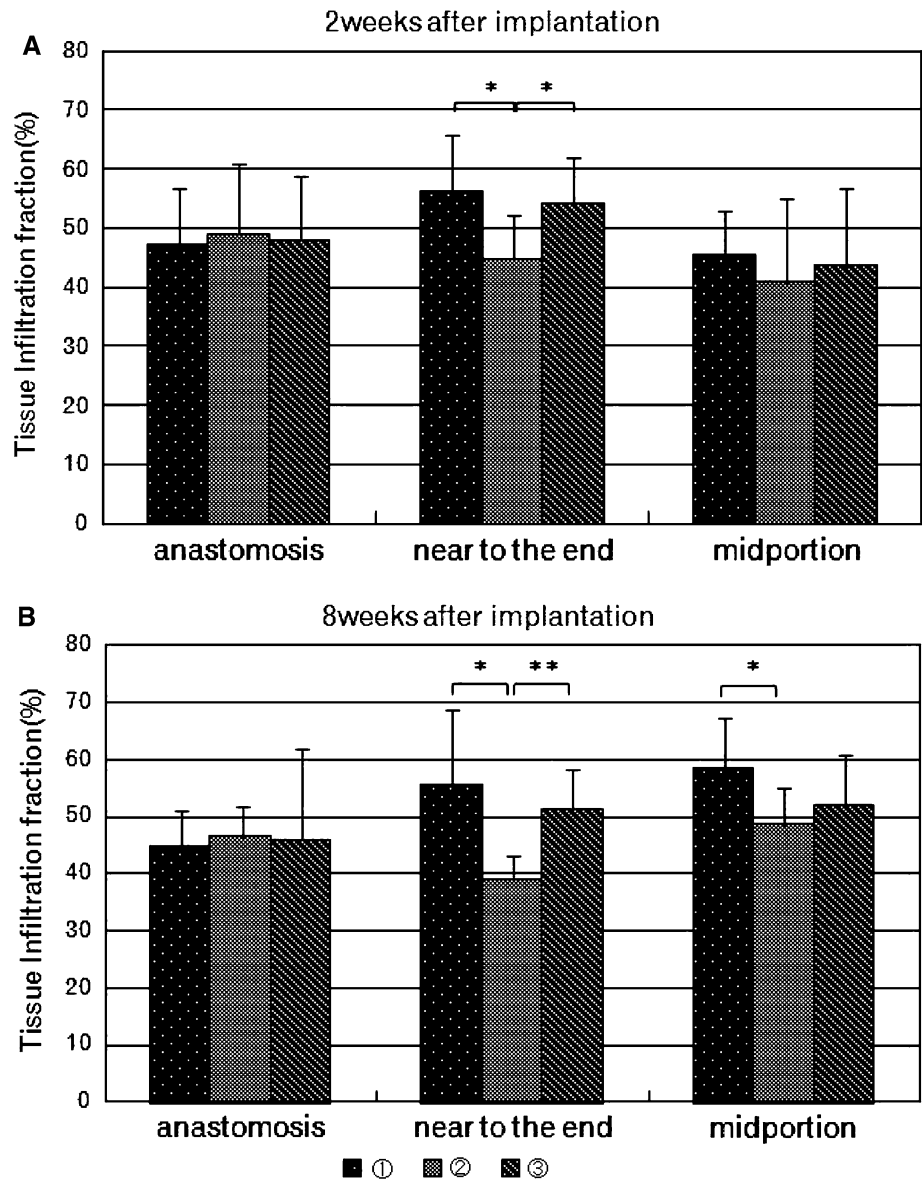
#### In vivo experiments with rats

Patency of the grafts except one (graft ③, 8 weeks after implantation) was observed by ultrasound Doppler flow study. Thus, we think the patency of our double-raschel silk fibroin grafts with coating is at least sufficient during 8 weeks after implantation. Examples of histological and immunohistological staining results are shown in Fig. 6. These were from one of the midportion cross-section of graft ①, 8 weeks after implantation. The lumen surface was stained with anti-CD31 antibody (Fig. 6a), and it shows that the lumen surface was covered with endothelial cells. Smooth muscle layer formation was observed on the

luminal side of the graft mainly by anti- $\alpha$ -SMA antibody (Fig. 6b). Figure 6c is the H&E staining image; we can see the tissue appearance from the picture.

At 2 weeks after implantation, endothelialization on the luminal surface of the graft was not complete: Endothelial cell coverage for grafts ①, ②, and ③ was  $37.1 \pm 11.9$ ,  $33.2 \pm 10.9$ , and  $39.2 \pm 8.0\%$ , respectively, in the midportion (Fig. 7). However, luminal surfaces from anastomosis to the midportion were completely covered with endothelial cells for most of the graft 8 weeks after implantation (Fig. 8). Different endothelial cell coverage among the three kinds of graft was not observed for both results 2 and 8 weeks after implantation.

**Fig. 10** Amount of tissue infiltration calculated from the images of H&E staining of three kinds of double-raschel bases 2 and 8 weeks after implantation. (\* $P < 0.05$ , \*\* $P < 0.01$ )



We measured the thickness of the smooth muscle layer formed on graft wall luminal side. Comparisons among the three kinds of grafts are shown in Fig. 9. At 2 weeks after implantation, no significant difference was identified, although a tendency to intimal hyperplasia appeared in grafts ② and ③. Graft ① had a smooth muscle layer thickness equal to that of the native aorta both 2 and 8 weeks after implantation.

In the H&E stained cross-section image, we measured the amount of tissue on the graft wall and regarded it as a marker of tissue infiltration or degradation. The large shift between 2 and 8 weeks after implantation was not shown clearly. Tissue infiltration into the wall of graft ② was lower than for grafts ① or ③ (Fig. 10).

**Discussion**

In this study, we developed small-diameter vascular grafts fabricated with silk fibroin and based on different types of double-raschel knitting. Silk fibroin has been reported as a biomaterial for regenerative medicine [14]; bone [15], cornea [16], etc., or drug-releasing scaffold [17]. These uses are based on high strength [9], biocompatibility [18], and biodegradation [19], etc. We prepared three kinds of knitted double-raschel silk fiber grafts, as bases for small-diameter vascular grafts, and coated these with cross-linked silk fibroin, by use of PGDE [20], to fabricate silk fibroin small-diameter vascular prostheses. The fabricated silk fibroin vascular grafts were evaluated by in-vitro physical property

testing and in vivo implantation testing in rats' aortas and the three kinds of double-raschel were compared.

In the physical property tests, it was shown that none of the silk fibroin grafts was less permeable and compressive than medical grade vascular prosthesis, when the permeability of fibroin grafts was compared with that of sealed polyethylene terephthalate prostheses [12], and the compressive strength of fibroin grafts was compared with a previous examination [13]. It was also observed that graft ① had greater elasticity than the other silk fibroin grafts. We considered that these results were derived from the closeness of the knitting and the thickness of the bases. The grafts implanted into rat abdominal aorta were almost free from thrombus formation during the study's observation period, except for one graft only, graft ③, 8 weeks after implantation. All the grafts withstood blood pressure and had not burst, because of the strength and toughness of silk fiber or coating [21].

The primary failure modes of artificial small-diameter vascular grafts are thrombus formation in the short term and intimal hyperplasia in the long term. Failure of these grafts has been attributed to compliance mismatch between rigid graft and elastic host artery and thrombogenicity of the blood-contacting surface of the synthetic grafts [22, 23]. In this study, therefore, we observed endothelialization and smooth muscle layer thickness on the luminal surface of the grafts by immunohistological staining using anti-CD31 and anti- $\alpha$ -smooth muscle actin (SMA) antibodies. The luminal surface of native vessels is covered with a layer of endothelial cells known to regulate thrombogenicity or intimal hyperplasia [23, 24]. In this study, almost all of the 7 mm length of the silk fibroin graft's luminal surface was covered with endothelial cells within 8 weeks of implantation, and the smooth muscle layer formed on luminal side of the wall of graft ① was as thick as that of the native aorta. A tendency to intimal hyperplasia was observed for grafts ② and ③. It was considered that these results were because of the bases' physical property difference, for example elasticity or flexibility. From H&E staining cross-section images we calculated the amount of tissue that penetrated the gaps between the knitting of the graft wall and regard it as tissue infiltration or degradation marker. But we could not identify significant differences between 2 and 8 weeks after implantation, so it was confirmed that 2 or 8 weeks were too short to replace the silk fibroin with autologous vessel.

In this study, we used rat a abdominal model to implant silk fibroin grafts based on double-raschel knitting and coated with cross-linked silk fibroin by use of PGDE. In the short term, the usefulness of the silk fibroin grafts was demonstrated, especially graft ①, because of its elasticity, flexibility, and inhibition of intimal hyperplasia. But the graft used in this study was short, so endothelial cells might

migrate easily and cover the graft luminal surface quickly. The silk fibroin fiber was not at all degraded in the 8-week implantation period. We need to optimize the endothelialization and degradation time of the silk fibroin grafts with longer length grafts and longer implantation times [1]. In the next step we are going to implant the silk fibroin graft in larger animals for further development of the clinical grade small-diameter vascular graft.

**Acknowledgments** TA acknowledges support from Grant from the Ministry of Agriculture, Forestry and Fisheries of Japan (Agri-Health Translational Research Project), Grant-in-Aid for Scientific Research from the Ministry of Education, Science, Culture and Sports of Japan (18105007), and Promotion of Basic Research Activities for Innovative Biosciences, Japan.

## References

1. Yokota T, Ichikawa H, Matsumiya G, Kuratani T, Sakaguchi T, Iwai S, Shirakawa Y, Torikai K, Saito A, Uchimura E, Kawaguchi N, Matsuura N, Sawa Y. In situ tissue regeneration using a novel tissue-engineered, small-caliber vascular graft without cell seeding. *J Thorac Cardiovasc Surg.* 2008;136:900–7.
2. Venkatraman S, Boey F, Lao LL. Implanted cardiovascular polymers: Natural, synthetic and bio-inspired. *Prog Polym Sci.* 2008;33:853–74.
3. Francois S, Chakfe N, Durand B, Laroche G. A poly(L-lactic acid) nanofibre mesh scaffold for endothelial cells on vascular prostheses. *Acta Biomater.* 2009;5:2418–28.
4. Schumann DA, Wippermann J, Klemm DO, Kramer F, Koth D, Kosmehl H, Wahlers T, Salehi-Gelani S. Artificial vascular implants from bacterial cellulose: preliminary results of small arterial substitutes. *Cellulose.* 2009;16:877–85.
5. Qiu YZ, Zhang N, Kang Q, An YH, Wen XJ. Fabrication of permeable tubular constructs from chemically modified chitosan with enhanced antithrombogenic property. *J Biomed Mater Res B Appl Biomater.* 2009;90B:668–78.
6. Liu Y, Vrana NE, Cahill PA, McGuinness GB. Physically crosslinked composite hydrogels of PVA with natural macromolecules: structure, mechanical properties, and endothelial cell compatibility. *J Biomed Mater Res B Appl Biomater.* 2009; 90B:492–502.
7. Mirensky TL, Nelson GN, Brennan MP, Roh JD, Hibino N, Yi T, Shinoka T, Breuer CK. Tissue-engineered arterial grafts: long-term results after implantation in a small animal model. *J Pediatr Surg.* 2009;44:1127–33.
8. Grasl C, Bergmeister H, Stoiber M, Schima H, Weigel G. Electrospun polyurethane vascular grafts: in vitro mechanical behavior and endothelial adhesion molecule expression. *J Biomed Mater Res A.* 2010;93A:716–23.
9. Altman GH, Diaz F, Jakuba C, Calabro T, Horan RL, Chen J, Lu H, Richmond J, Kaplan DL. Silk-based biomaterials. *Biomaterials.* 2003;24:401–16.
10. Enomoto S, Sumi M, Kajimoto K, Nakazawa Y, Takahashi R, Takabayashi C, Asakura T, Sata M. Long-term patency of small-diameter vascular graft made from fibroin, a silk-based biodegradable material. *J Vasc Surg.* 2010;51:155–64.
11. Pektok E, Cikirikcioglu M, Tille JC, Kalangos A, Walpoth BH. Alcohol pretreatment of small-diameter expanded polytetrafluoroethylene grafts: quantitative analysis of graft healing characteristics in the rat abdominal aorta interposition model. *Artif Organs.* 2009;33:532–7.

12. CDRH. Guidance for industry and FDA staff guidance document for vascular prostheses. 1999.
13. Hayashi F, Okuda Y, Nakata M, Natori K. Development of small-diameter ePTFE vascular graft. *SEI Tech Rev.* 2002;161:102–6.
14. Minoura N, Aiba S, Gotoh Y, Tsukada M, Imai Y. Attachment and growth of cultured fibroblast cells on silk protein matrices. *J Biomed Mater Res.* 1995;29:1215–21.
15. Sofia S, McCarthy MB, Gronowicz G, Kaplan DL. Functionalized silk-based biomaterials for bone formation. *J Biomed Mater Res.* 2001;54:139–48.
16. Lawrence BD, Marchant JK, Pindrus MA, Omenetto FG, Kaplan DL. Silk film biomaterials for cornea tissue engineering. *Biomaterials.* 2009;30:1299–308.
17. Mandal BB, Kundu SC. Calcium alginate beads embedded in silk fibroin as 3D dual drug releasing scaffolds. *Biomaterials.* 2009;30:5170–7.
18. Meinel L, Hofmann S, Karageorgiou V, Kirker-Head C, McCool J, Gronowicz G, Zichner L, Langer R, Vunjak-Novakovic G, Kaplan DL. The inflammatory responses to silk films in vitro and in vivo. *Biomaterials.* 2005;26:147–55.
19. Horan RL, Antle K, Collette AL, Huang YZ, Huang J, Moreau JE, Volloch V, Kaplan DL, Altman GH. In vitro degradation of silk fibroin. *Biomaterials.* 2005;26:3385–93.
20. Min SJ, Gao X, Liu L, Tian L, Zhu LJ, Zhang HP, Yao J. Fabrication and characterization of porous tubular silk fibroin scaffolds. *J Biomater Sci Polym Ed.* 2009;20:1961–74.
21. Zhao CH, Yao JM, Masuda H, Kishore R, Asakura T. Structural characterization and artificial fiber formation of *Bombyx mori* silk fibroin in hexafluoro-iso-propanol solvent system. *Biopolymers.* 2003;69:253–9.
22. Abbott WM, Megerman J, Hasson JE, Litalien G, Warnock DF. Effect of compliance mismatch on vascular graft patency. *J Vasc Surg.* 1987;5:376–82.
23. Losi P, Lombardi S, Briganti E, Soldani G. Luminal surface microgeometry affects platelet adhesion in small-diameter synthetic grafts. *Biomaterials.* 2004;25:4447–55.
24. Sarkar S, Sales KM, Hamilton G, Seifalian AM. Addressing thrombogenicity in vascular graft construction. *J Biomed Mater Res B Appl Biomater.* 2007;82B:100–8.